Identification of the binding site for ammonia in GMP reductase

Master's Thesis

Presented to

The Faculty of the Graduate School of Arts and Sciences
Brandeis University
Department of Biology
Lizbeth Hedstrom, Advisor

In Partial Fulfillment
of the Requirements for the Degree

Master of Science
in
Molecular and Cell Biology

by
Tianjiong Yao

February 2015

ABSTRACT

Identification of the binding site for ammonia in GMP reductase

A thesis presented to the Department of Biology

Graduate School of Arts and Sciences
Brandeis University
Waltham, Massachusetts

By Tianjiong Yao

The overall reaction of guanosine monophosphate reductase (GMPR) converts GMP to IMP by using NADPH as a cofactor and it includes two sub-steps: (1) a deamination step that releases ammonia from GMP and forms the intermediate E-XMP*; (2) a hydride transfer step that converts E-XMP* to IMP along with the oxidation of NADPH. The hydride transfer step is the rate limiting step, yet we failed to observe a burst of ammonia release. Meanwhile ammonia cannot stay in the same place where it is formed otherwise it will block NADPH. This observation suggests that ammonia remains bound to the enzyme during the hydride transfer step and there exists ammonia holding site after its release from the formation site. We identified a possible ammonia holding site by inspection of crystal structure of human GMPR type 2. Three candidate amino acids were selected and probed by site directed mutagenesis. The substitutions of all three residues decreased the reduction of GMP at least 50 fold and the oxidation of IMP at least 40 fold, and reduced the intermediate production at least 2 fold. Therefore, these substitutions behave as expected for mutations at the ammonia holding site.

Table of Contents:

List of Tables:

List of Figures:

I. Introduction:

How structure determines enzyme function or how subtle structural changes vary the reaction outcomes remain one of the central conundrums in biochemistry and structural biology. The approach to these questions also provides a new insight into determinants of reaction specificity in different enzymes with similar structures. The findings of these questions can give an extensive application such as predicting the consequences of enzyme mutations, thus offering promising usage in future enzyme redesign and drug industry.

This central challenge remaining in biochemistry can be illustrated by $(\beta\text{-}\alpha)_8$ barrel proteins, also known as TIM barrels. This kind of fold is the most common structure among enzyme structures, and over thirty $(\beta\text{-}\alpha)_8$ proteins superfamilies are recorded in the current Structural Classification of Proteins (SCOP) and CATH databases. Also, this structure is the most versatile protein fold catalyzing over twenty five different reactions (L. Hedstrom, 2012). Two enzymes that belong to the same superfamily in $(\beta\text{-}\alpha)_8$ barrel proteins prove to be an excellent model to study the reaction specificity----inosine monophosphate dehydrogenase (IMPDH) and guanosine monophosphate reductase (GMPR). IMPDH and GMPR have about 30% sequence identity and share a common set of catalytic residues. They bind ligands with similar affinities and catalyze similar reactions but in different directions (Gregory C Patton *et al.*, 2011).

IMPDH catalyzes the oxidation of IMP into XMP with the reduction of cofactor NAD^+. IMP

is the product of the *de novo* purine biosynthesis pathway and most organisms can also produce IMP via salvage pathways. So IMPDH serves as an important catalytic enzyme in both pathways (Figure 1). The XMP production catalyzed by IMPDH is the first committed step in guanine nucleotide biosynthesis and thus the major role of IMPDH is the expansion of guanine nucleotide pool for proliferation. So, all these characteristics make IMPDH an invaluable target for immunosuppressive, antiviral and anticancer drugs (L. Hedstrom, 2009). On the other hand, GMPR catalyzes the reduction of GMP into IMP and ammonia with the oxidation of cofactor NADPH (Figure 1). So, GMPR plays a significant role in the conversion of guanine nucleotides into adenine nucleotides and thus regulates guanine nucleotide pool as well (Jixi Li *et al.*, 2005). In addition, human GMPR type 2 has been acknowledged to promote monocytic differentiation of HL-60 leukemia cells (Jia Zhang *et al.*, 2003). Recent research has also shown that GMPR downregulates the amounts of several GTP-bound (active) Rho-GTPases and suppresses the invasion of melanoma cells (Joseph A. Wawrzyniak *et al.*, 2013). All these findings make GMPR equally an interesting and promising object to study.

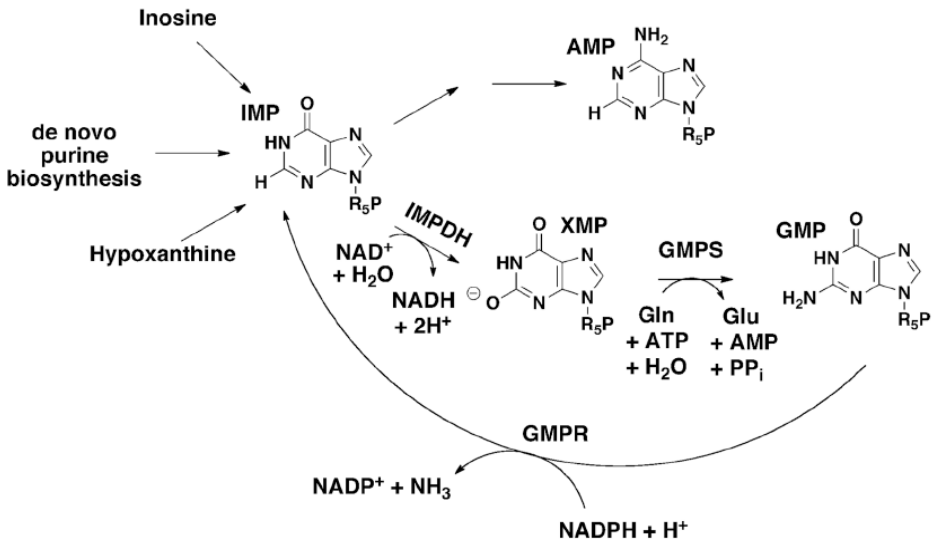

Figure 1: Purine Nucleotide Metabolism (L. Hedstrom, 2012). GMP synthetase (GMPS) catalyzes the subsequent conversion of XMP to GMP. The abbreviation "R5P" stands for the remaining structure of GMP (Appendices: GMP structure).

The whole catalytic reaction for both enzymes includes two separate steps. In the case of IMPDH, these reactions are: (i) a hydride transfer reaction that produces NADH and the covalent intermediate E-XMP* and (ii) a hydrolysis reaction that releases XMP. In contrast, GMPR catalyzes: (i) a deamination step that releases ammonia from GMP and forms the intermediate E-XMP*; (ii) a hydride transfer step that converts E-XMP* to IMP utilizing NADPH as a cofactor (L. Hedstrom, 2012). The problem of how a single active site catalyzes two different chemical reactions has been solved in two different ways (Figure 2): the IMPDH reaction uses two different protein conformations (open and closed) to catalyze the two different chemical transformations, whereas GMPR uses two different cofactor (NADPH) conformations (out and in). Furthermore, the latest research showed the evidence that GMPR was also capable of shifting the equilibrium towards the partial backward direction, that means the enzyme can form E-XMP* and release NADPH in the presence of only IMP and $NADP^+$ (Gregory C Patton *et al.*, 2011). Both reactions catalyzed by IMPDH and GMPR

involve the same intermediate E-XMP*, but E-XMP* reacts with water in IMPDH via Arg418-Tyr419 dyad and it reacts exclusively with ammonia in GMPR via Thr188-Glu289 dyad, then resulting in different final outcomes (Gregory C Patton *et al.*, 2011). Moreover, the proposed mechanism has showed that when ammonia is produced, it needs to leave the active site otherwise it will block NADPH binding, thus preventing the following reaction (Figure 3). So, here emerges the question: what causes this reaction specificity between two similar structure enzymes?

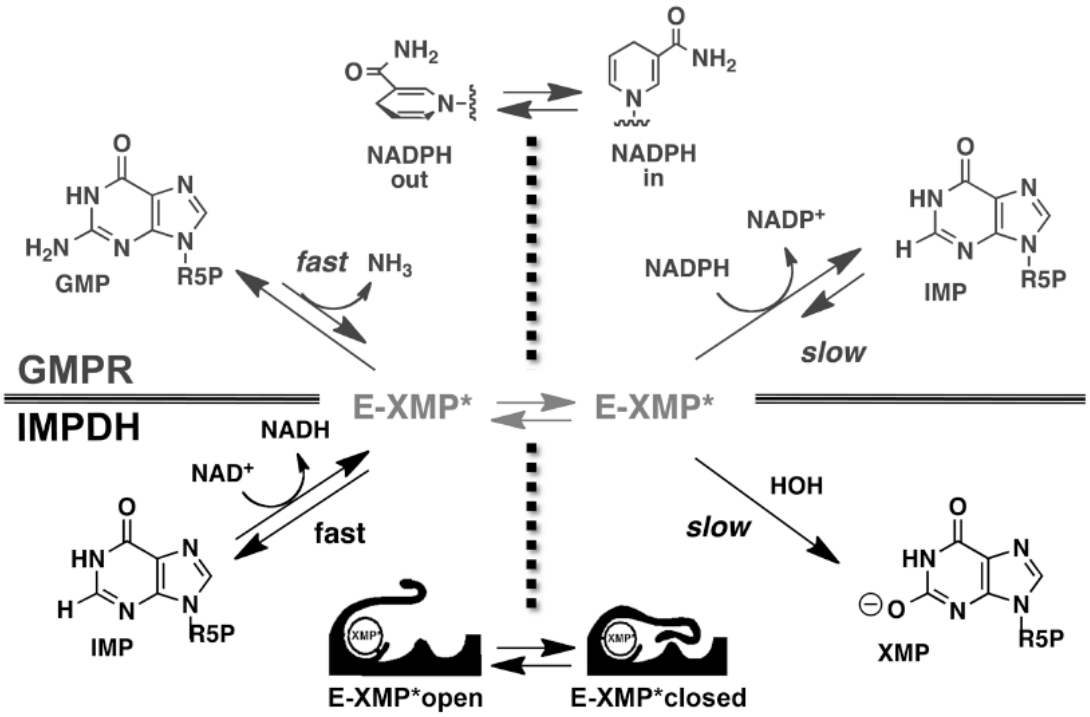

Figure 2: The Mechanisms of IMPDH and GMPR (L. Hedstrom, 2012). Previous proposed model, the ammonia actually leaves at end of the whole GMPR reaction.

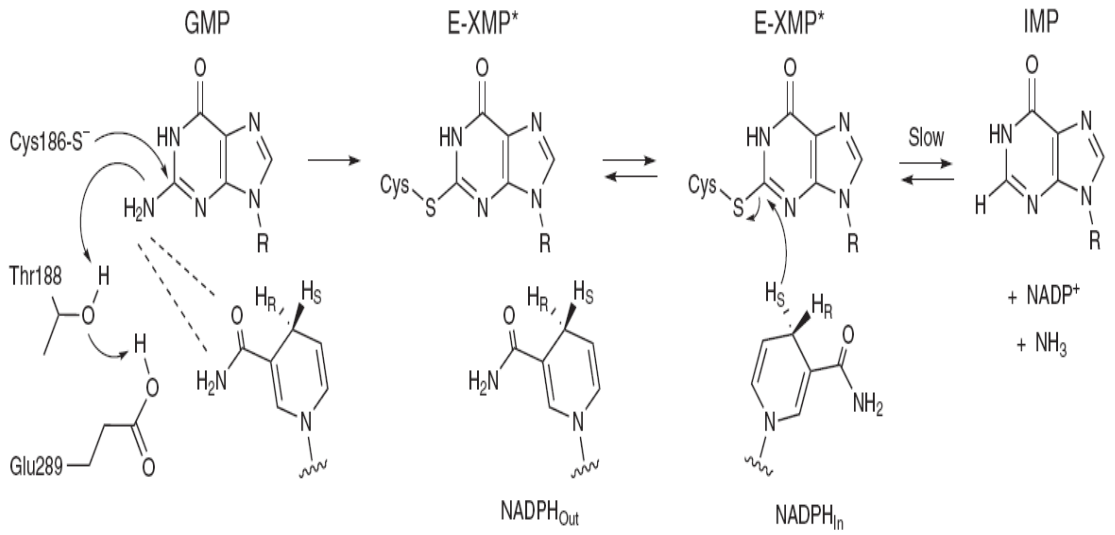

Figure 3: The Mechanism of GMPR (Gregory C Patton *et al.*, 2011)

As we know, the hydride transfer step is the rate limiting step in GMPR reaction, yet we failed to observe a burst of ammonia release in wild type GMPR from previous research data. This observation suggests that ammonia remains bound to the enzyme during the hydride transfer step in GMPR and there exists ammonia holding site after its release form the formation site. So, identification of possible ammonia holding sites in GMPR may help to reveal the mystery of substrate specificity between IMPDH and GMPR: water or ammonia. Here we present the results of testing three candidate residues with four different substitutions: T188A, Y318A, Y318F and A131Q. The substitutions decrease the deamination step but have little effect on hydride transfer step, and both steps can make intermediate complex depending on the direction considered. All three replaced residues decrease the reduction of GMP at least 50 fold and the oxidation of IMP at least 40 fold, and reduce the intermediate production at least 2 fold in hydride transfer step. Thus, by selecting the candidate amino acid as the holding site in GMPR, a further research can be carried out to look into the similar amino acid sequence structure in IMPDH.

II. Results and Discussion:

1. Structure overview and selection of candidate residues:

GMPR is homotetramer, with the catalytic $(\beta\text{-}\alpha)_8$ barrels arranged in square planar geometry. All our following experiments used *E. coli* GMPR (EcGMPR), but unfortunately there is no available crystal structure data of EcGMPR currently, so we inspected the crystal structure of human GMPR type 2 (hGMPR2) instead (hGMPR2: PDB code 2C6Q). The sequences of hGMPR2 and EcGMPR are 69% identical overall, and the active site residues are completely conserved. Both EcGMPR and hGMPR2 crystals contained two tetramers in the asymmetric unit (tetramer 1, subunits A–D; tetramer 2, subunits E–H). The monomers had the expected $(\beta\text{-}\alpha)_8$ barrel structure. We observed the structures of hGMPR2 in an E–IMP–NADPH ternary complex at 1.7-Å resolution in order to gain insight into the structural basis of reaction specificity in EcGMPR.

Among all eight subunits, half of them (subunit A, D, E, H) have “out” conformation NADPH and the other half (subunit B, C, F, G) have “in” conformation NADPH. All eight subunits have almost same conformation, so here we only show structures of two subunits each presenting a different conformation of NADPH (Figure 4).

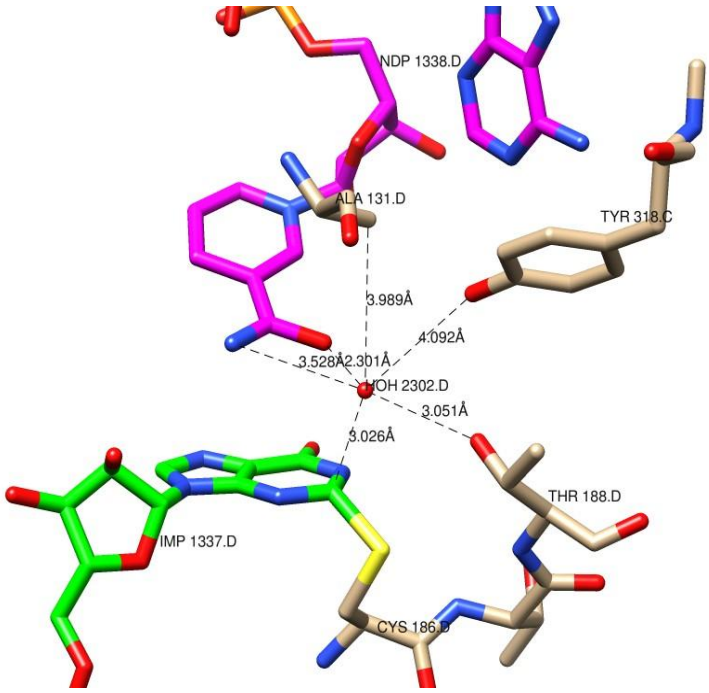

(a) “out” conformation of NADPH in subunit D in hGMPR2 and partial subunit C (Tyr318)

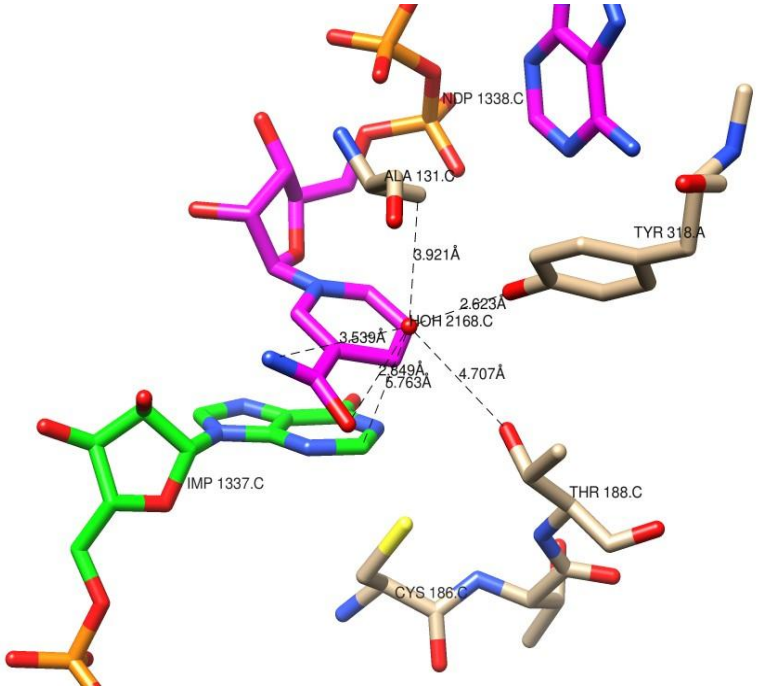

(b) “in” conformation of NADPH in subunit C in hGMPR2 and partial subunit A (Tyr318)

Figure 4: Structure of E-IMP-NADPH complex (PDB code 2C6Q). Figures (a) and (b) were rendered with Chimera.

As shown in the figure 4 (a), electron density modeled as H_2O is hypothesized to be in the position where NH_3 should leave after Cys186 attacks the C2 site of GMP. In the figure 4 (b), electron density modeled as H_2O is hypothesized to be in the position where NH_3 being held during the hydride transfer step. So the crystal model suggests that this water molecule could represent NH_3 considering their similar chemical properties. According to the distance analysis between this modeled water molecule and its nearby residues, the results give us several interesting thoughts:

First of all, this water molecule has a distance of 3.5 Å to Thr188 in “out” conformation and it expands to 4.7 Å in “in” conformation. This means in “out” conformation Thr188 can form a hydrogen bond with ammonia that can possibly hold ammonia when its release during the deamination step, but there is no hydrogen bond between ammonia and Thr188 in “in” conformation during the hydride transfer step. Considering that Thr188-Glu289 dyad plays an important role in deamination step in GMPR reaction, and previous research reports that Thr188 is required for donating electron during deamination step. Thr188 could be a good candidate for holding ammonia. But still, ammonia remains bound to enzyme during the whole GMPR reaction that means we need to find other residue that can possibly hold ammonia during the hydride transfer step. So in our experiment, we mutated Thr188 to Ala188 to see if this mutation will affect the reaction rate.

Second, this water molecule has a distance of 4.1 Å to Tyr318 in “out” conformation and it decreases to 2.6 Å in “in” conformation. That predicts that Tyr318 has barely no effect on ammonia during the deamination step, but it can form a strong hydrogen bond to ammonia during the hydride transfer step. This observation makes Tyr318 an even more interesting

candidate residue for holding ammonia because it compensates the fact that Thr188 cannot form a hydrogen bond to ammonia during the hydride transfer step. One more interesting thing to mention is that Tyr318 doesn't belong to local subunit; it actually comes from other subunit. For instance, as shown in figure 4 (a) and 4 (b), in subunit D, Tyr318 comes from subunit C; in subunit C, Tyr318 comes from subunit A. So, in other subunits, Tyr318 also comes from its nearby subunit. This observation implies that Tyr318 might have some special usage that can compensate local subunit catalytic function. So in our experiment, we mutated Tyr318 into two different residues: Phe318 and Ala318. On one hand, the Phenyalanine residue conserves the aromatic ring and it has almost same structure to Tyrosine except one hydroxyl group. On the other hand, the alanine residue completely changes the structure at this site.

Last but not least, this water molecule has a distance of 3.9 Å to Ala131 in "out" conformation and the distance barely changes anything in "in" conformation. Because this residue stays a constant distance to ammonia and seems to have no direct influence on it in both deamination and hydride transfer steps, we mutated this residue Ala131 to Gln131 in order to have a longer side chain that could possibly block the ammonia binding site. According to the crystal model, the new residue with a longer side chain could "push" away the ammonia from its original release position as shown in the figure, so the ammonia will probably not be held by any residue thus being released faster than the whole reaction. If this mutation worked as we expected, that means this selected ammonia has a very high chance being the "released" ammonia and justifies the above two selected residues (Thr188 and Tyr318) with respect to their distances of hydrogen bonds to the "released" ammonia.

2. Steady State Kinetics:

EcGMPR	Forward Reaction (GMP+NADPH)		
	Km(μM) of GMP	Km(μM) of NADPH	kcat(s^{-1})
WT	3.2 ± 0.5	10.1 ± 0.8	0.35 ± 0.01
T188A	41 ± 22	137 ± 113	0.003 ± 0.001
Y318A	55 ± 13	201 ± 86	0.0025 ± 0.0006
Y318F	29 ± 7	1455 ± 3458	0.52 ± 0.01
A131Q	12 ± 3	167 ± 86	0.007 ± 0.001

(a) kinetic parameters for forward reaction

EcGMPR	Backward Reaction (IMP+$NADP^+$+NH_3)		
	Km(μM) of IMP	Km(μM) of $NADP^+$	kcat(s^{-1})
WT	23 ± 6	50 ± 16	0.018 ± 0.009
T188A	B.D.	B.D.	B.D.
Y318A	B.D.	B.D.	B.D.
Y318F	32 ± 8	90 ± 13	(4.5 ± 0.5) x 10^{-4}
A131Q	B.D.	B.D.	B.D.

(b) kinetic parameters for backward reaction

Table 1: Kinetic Parameters of wild-type GMPR and mutations: kcat in forward reaction is calculated by GMP consumption; kcat in backward reaction is calculated by IMP consumption. B.D. stands for below detection (the corresponding activity was < 0.5% of WT activity). All reactions were conducted for over 30 minutes at 25°C. Buffer (75mM Tris pH 7.8, 100mM KCl, 1mM EDTA and 1mM DTT). [GMP]=10μM-160μM, [NADPH]=10μM-160μM. [IMP] varies from 20μM to 640μM, when fixing [$NADP^+$]=1mM, [NH_4^+]=20mM; [$NADP^+$] varies from 20μM to 640μM, when fixing [IMP]=1mM, [NH_4^+]=20mM.

In order to see kinetics parameters of WT and all mutants in steady state, we performed both forward reaction and backward reaction for WT and all mutants. Because all cuvettes we used have a diameter of 1cm and the absorbance measured by spectrophotometer should be between 0.1-1.0, according to the Lambert-Beer Law, the maximum concentration of NADPH we can apply for the forward reaction is 160μM and it is still not enough for saturation (see Table 1a). So we conducted a matrix measurement for all mutants via varying GMP concentration from 10μM to 160μM and NADPH concentration from 10μM to 160μM. The kinetics data of WT was collected from previous paper (Gregory C Patton *et al.*, 2011). As for the backward reaction, Km of IMP was calculated by varying the concentration of IMP from 20μM to 640μM in the presence of 1mM $NADP^+$ and 20mM NH_4^+, and Km of $NADP^+$ was calculated by varying the concentration of $NADP^+$ from 20μM to 640μM in the presence of 1mM IMP and 20mM NH_4^+.

For the starter, the WT data was collected from previous paper who conducted the measurement by saturating the NADPH (1mM) and varying the GMP concentration, whereas all the data of mutants were collected by matrix measurement that will expand the final value. Because the actual data are expanded by extrapolation, we can consider that kcat of WT and kcat of Y318F are within the same range. That means the substitution of Tyr318 to Phe doesn't change too much the reaction rate for the forward reaction. However, at the same position, a different substitution of Tyr318 causes a huge difference. The kcat of Y318A is over 100 fold less than the kcat of WT meaning that (i) Tyr318 is supposed to promote the forward reaction and (ii) the aromatic ring of Tyr318 is mainly responsible for maintaining its catalytic function. Despite the extrapolation fact, the kcat of T188A is still at least 100 fold

less than kcat of WT, and the kcat of A131Q is 50 fold less. That means Thr188 plays a significant role in the forward reaction especially in deamination step as reported before. The interesting finding is that when “pushing” ammonia away from its original release site by longer side chain of A131Q, the reaction velocity is slowed, meaning that the ammonia should be held someplace inside enzyme otherwise it will interrupt the reaction rate. Another possible explanation for the result of A131Q is that this substitution will block the cofactor (NADPH) from establishing the “out” conformation thus slowing down the forward reaction rate.

Furthermore, we tested the ability of different kinds of GMPR to catalyze the conversion of IMP in the presence of $NADP^+$ and NH_3. The reactions were below detection for mutants T188A, Y318A and A131Q (All of their activities were < 0.5% of the activity of wild-type GMPR). The measuring methods of WT and Y318F are the same, and the kcat of Y318F is 40 fold less than the kcat of WT. A mutation must affect the forward and backward reaction by the same amount, but in contrast to the forward reaction, the substitution of Tyr318 to Phe does reduce the rate of whole backward reaction with a higher fold. This can be explained that Tyr318 only affects the deamination step (partial reaction) and its aromatic ring structural is important during this step. Moreover, by comparing the result of Y318F and Y318A, it shows further that Tyr318 does have a huge influence on ammonia holding during the backward reaction, and the aromatic ring of residue is the key point in the reaction. As for the observations of T188A and A131Q, they are consistent to the previous results from forward reaction. That means Thr188 also contributes to the backward reaction, but since Thr188 has been reported being a main component for activating deamination step, more

tests will be carried out. The discovery of A131Q, on the other hand, further indicates the same imply form the forward reaction: the original release site of ammonia is very important, if it is pushed away, the ammonia can no longer be held by the nearby residues thus preventing the backward reaction. This implication verifies the selection of two previous candidate residues: Thr188 and Tyr 318.

In order to gain more insight to the function change with reference to the different substitution, we performed pre-steady state kinetic assays by stopped flow.

3. Pre-steady State Kinetics:

(1) Proton uptake--control experiments and assays:

In order to verify the ability of stopped flow that it can measure the proton uptake extent according to the absorbance change, we performed several control experiments to present the result by using Phenol Red as the indicator and reading the absorbance at 560nm wavelength. The following charts show the control result for proton uptake assay.

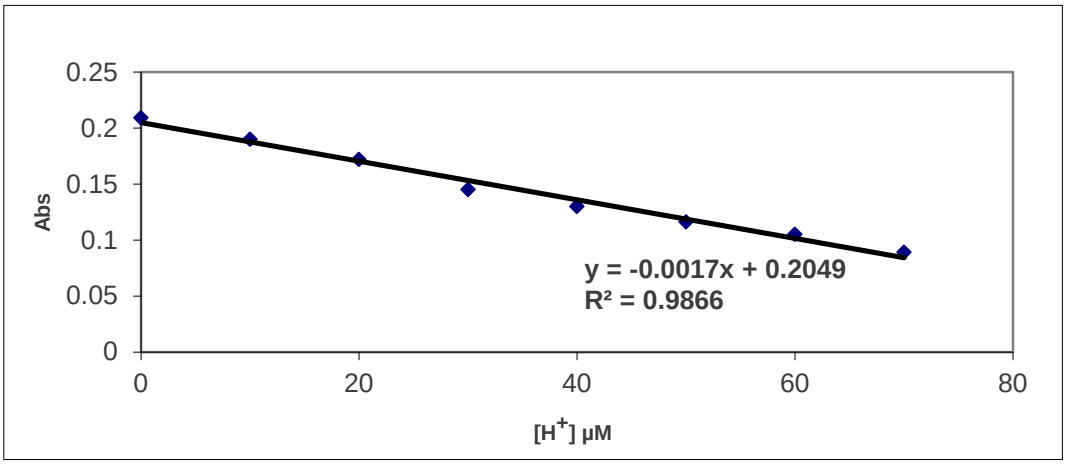

(a) Absorbance change with respect to pH change by adding H^+

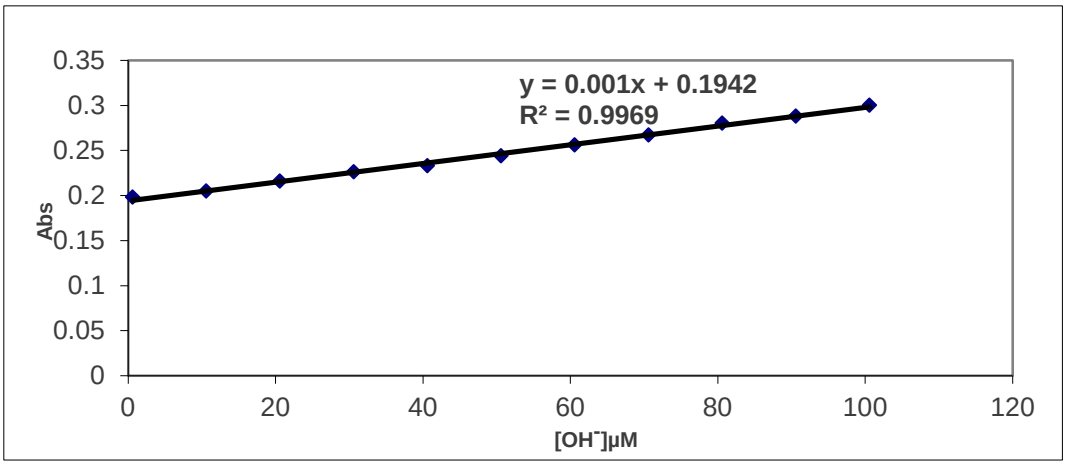

(b) Absorbance change with respect to pH change by adding OH^-

Figure 5: Proton uptake control groups: absorbance changes within the change of pH. The indicator (phenol red) will change its color with reference to the change of environmental pH, and its color change will result in an absorbance change. 30μL of 1mM indicator (phenol red) is added into 1mL buffer (0.5mM Tris pH 7.8, 150mM KCl, 1mM DTT). Absorbance read at 560nm wavelength.

As the Figure 5 shows, the stopped flow assay can sensitively measure the pH change and reflect the corresponding result by showing the changing absorbance. When the deamination step is completed in the forward GMPR reaction, the NH_3 is released and it will take the proton form the surrounding environment and cause an accumulation of OH^-. So, we can know the release amount of NH_3 per time unit by measuring the absorbance change. Then, after confirming the ability of stopped flow assay, we performed the proton uptake assays and the backward reactions (both partial and whole) for WT GMPR and all mutants.

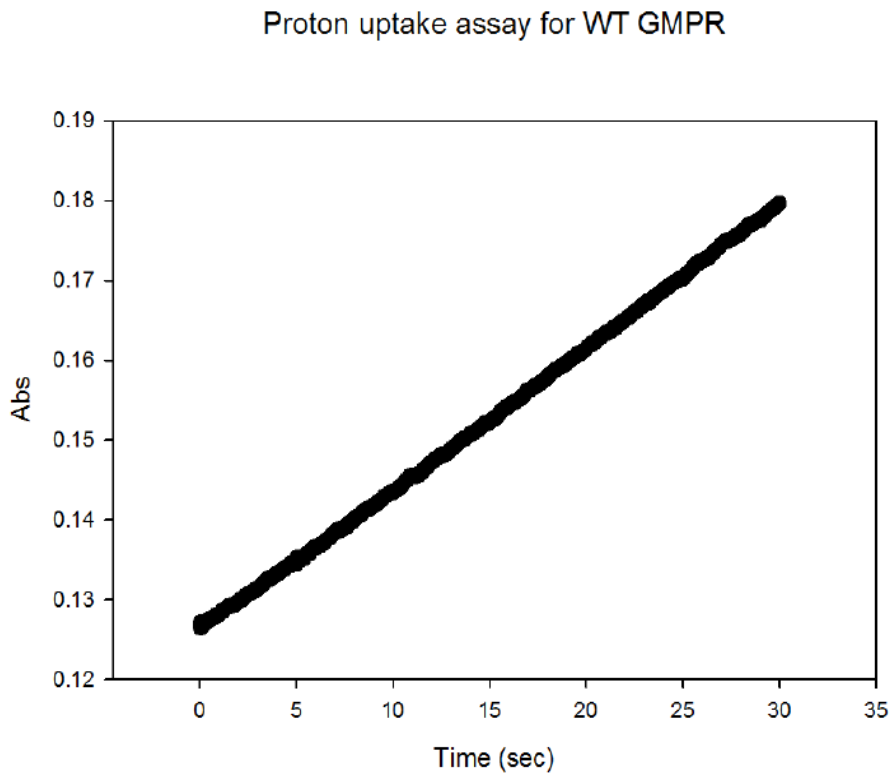

(a)Proton uptake assay for WT GMPR

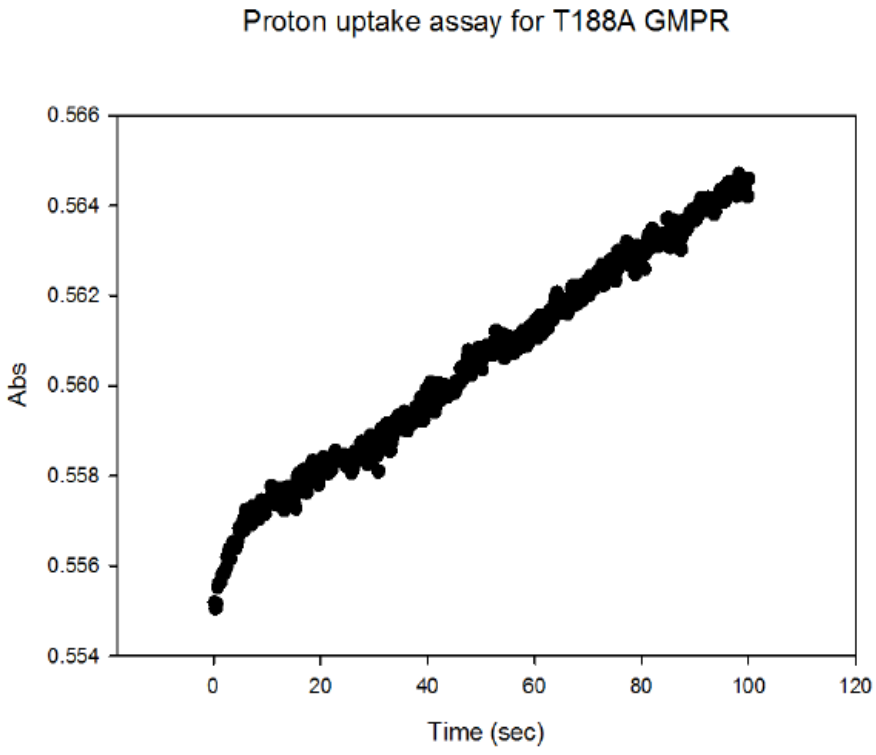

(b) Proton uptake assay for T188A GMPR

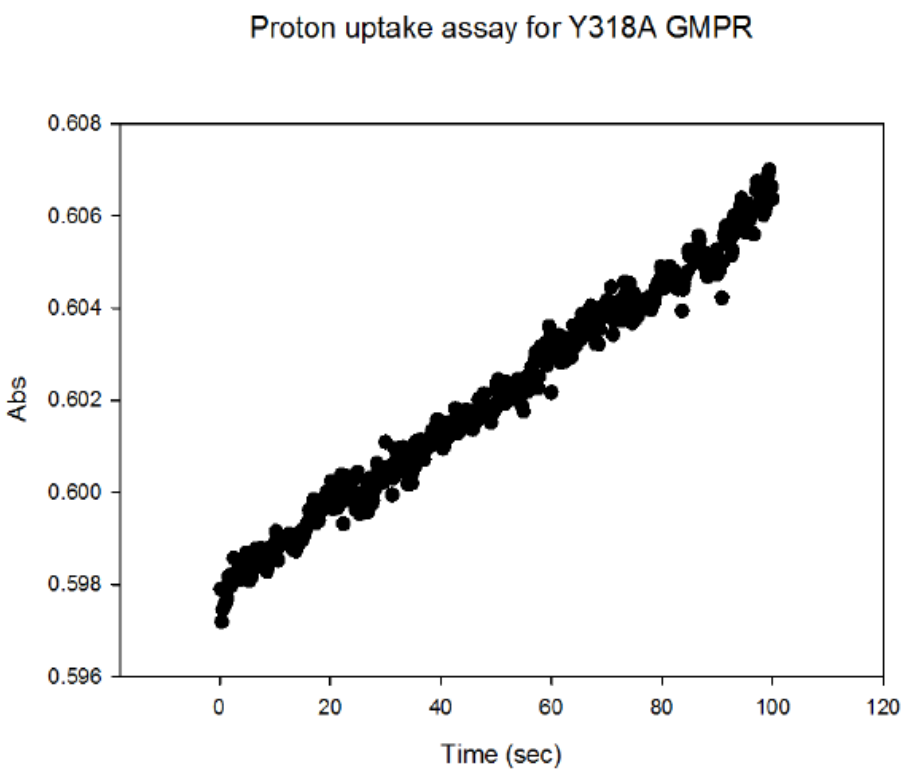

(c) Proton uptake assay for Y318A GMPR

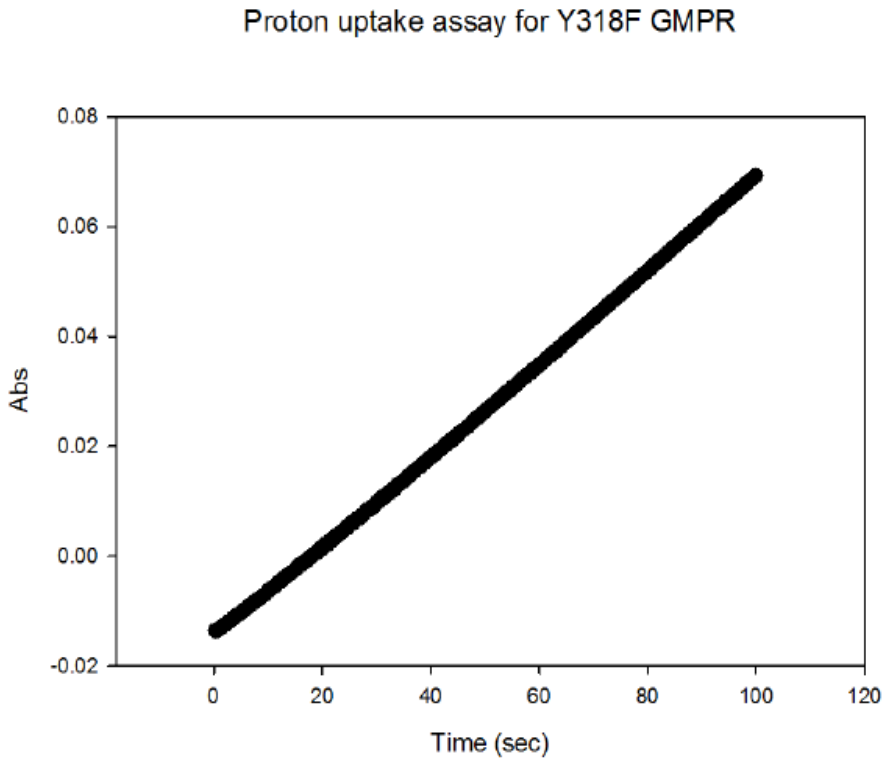

(d) Proton uptake assay for Y318F GMPR

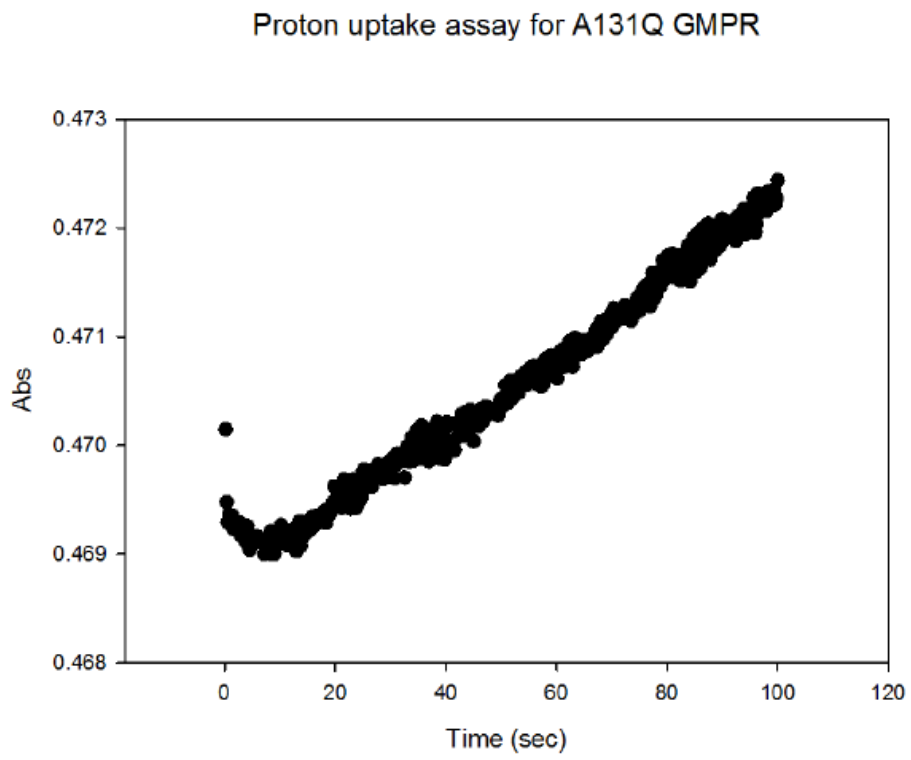

(e) Proton uptake assay for A131Q GMPR

Figure 6: Proton uptake assays for WT GMPR and all mutants. 30µL of 1mM indicator (phenol red) is added into 1mL buffer (0.5mM Tris pH 7.8, 150mM KCl, 1mM DTT). [GMP]=500µM, [NADPH] =500µM. The absorbance is read at 560nm wavelength for 100 seconds (for WT only 40s) at 25^{o}C. Each figure presents a different enzyme concentration in experiment: (a) [WT]=10µM; (b) [T188A]=30µM; (c) [Y318A]=30µM; (d) [Y318F]=10µM; (e) [A131Q]=10µM.

According to the Figure 6 (a), since we already know that the hydride transfer is the rate limiting step in the whole GMPR reaction and the proton uptake result of WT show a linear increase instead of an exponential burst followed by a linear steady state. Also, the kcat of proton uptake for WT is 0.36±0.01 s^{-1} which is almost identical to the kcat (0.35±0.01 s^{-1}) of whole forward reaction, indicating that there is no significant difference between the rates of deamination step and the whole forward reaction. That means ammonia remains bound to enzyme during the whole forward reaction even after its original release from the deamination step.

Figure 6 (b) shows the proton uptake result of T188A. The curve has a small burst at the beginning 5 seconds of the whole measurement, and the production is about 13% relative to the enzyme active sites. The small burst presents the pre-steady state in which ammonia is released faster than hydride transfer, indicating that the hydride transfer step is the rate limiting step. The different pre-steady state between WT and T188A shows that the substitution of Thr188 can actually accelerate ammonia release. However, the kcat of proton uptake for T188A is 0.0056±0.0001 s^{-1}, which is very close to the kcat of the whole forward reaction for T188A which is 0.003±0.001 s^{-1}. So, even though the substitution of Thr188 can jeopardize the ammonia holding to some extent in the pre-steady state, but overall, it is still not enough for releasing a big amount of ammonia implying that other sites may help to hold ammonia as well. Also, previous report stated that Thr188 was supposed to donate the proton for the deamination step, this substitution means the ammonia is still released without Thr188 donation. This discovery means that Thr188 has two functions: donate proton for deamination step and hold ammonia during the deamination step.

Figure 6 (c) shows the proton uptake result of Y318A. The curve has a tiny burst at the beginning 3 seconds of the whole measurement, and the production is about 7% relative to the enzyme active sites. The different pre-steady state between WT and Y318A shows that the substitution of Tyr318 can also make ammonia being released a little faster. The kcat of proton uptake for Y318A is 0.0055±0.0001 s^{-1}, which is also very close to the kcat of the whole forward reaction for Y318A is 0.0025±0.0006 s^{-1}. The overall result shows a similar conclusion as T188A does: the substitution of Tyr318 can release a certain level of ammonia faster in the pre-steady state, but itself is not enough for holding all the ammonia.

Figure 6 (d) shows that, for Y318F, the rates of deamination step and the whole forward reaction are very close, and the proton uptake kcat (0.17±0.01 s^{-1}) and kcat of whole forward reaction (0.52±0.01 s^{-1}) further confirm that. So we can consider that substitution Y318F won't affect the ammonia releasing rate. The curve of Y318F is very similar to the curve of WT GMPR (without any burst at the beginning) but differs from the curve of Y318A (with a small burst at the beginning) meaning that the aromatic ring in Tyr318 is the key point in keeping ammonia inside the enzyme during the reaction.

Figure 6 (e) shows there is a small decrease at the beginning of the whole reaction of A131Q but shows no burst. That means somehow the enzyme releases protons first to provide an appropriate surrounding environment for deamination, then it proceeds to carry out the forward reaction. One possible explanation is that the longer side chain of Gln131 blocks the environmental proton sources (like Thr188, etc.) whereas the deamination step requires extra proton to finish ammonia releasing, so the mutant enzyme itself produces protons to ensure the continuation of deamination step. Anyway, there is no burst at the beginning indicating that ammonia is not released before the hydride transfer step in the pre-steady state. The proton uptake kcat (0.0072±0.0001 s^{-1}) is very close to the kcat (0.007±0.001 s^{-1}) of the whole forward reaction. That means the substitution A131Q won't change the overall forward reaction rate.

(2) Backward Reaction--partial and whole reaction:

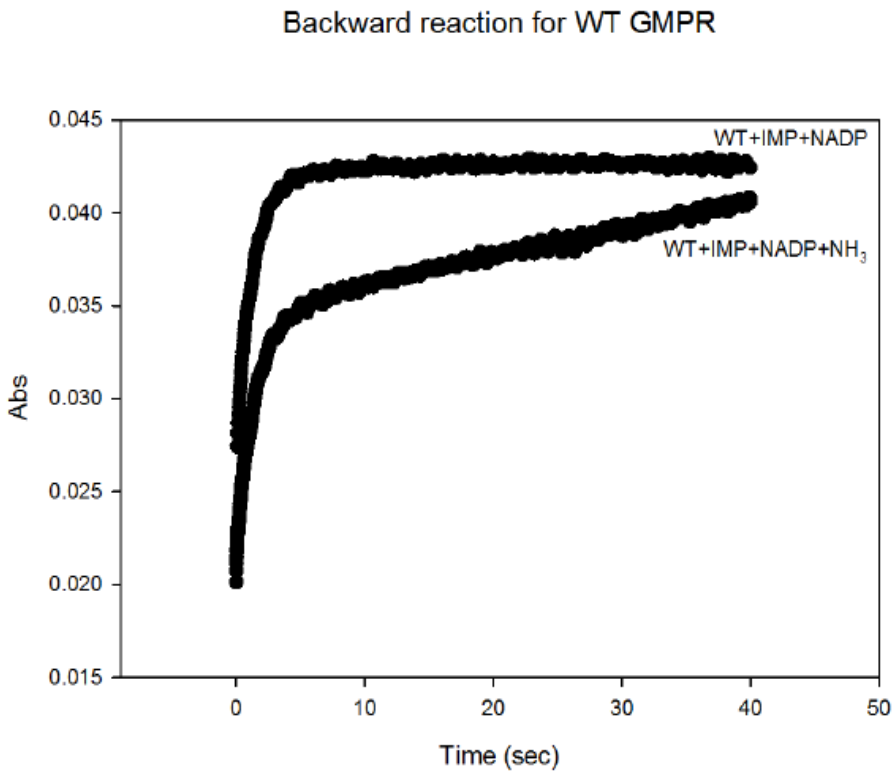

(a)Backward reaction for WT GMPR

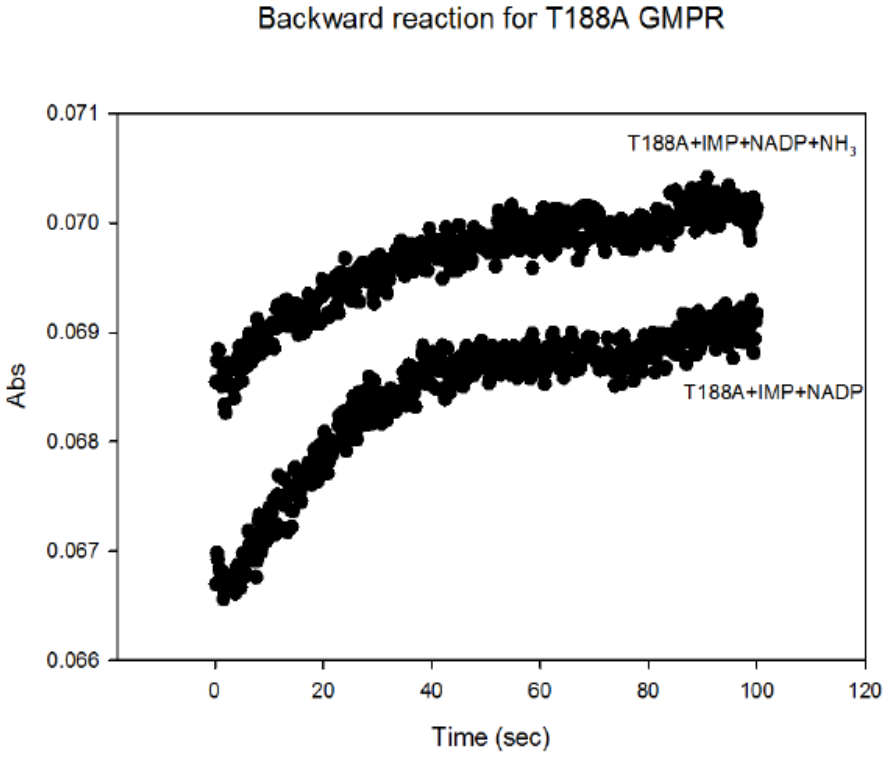

(b) Backward reaction for T188A GMPR

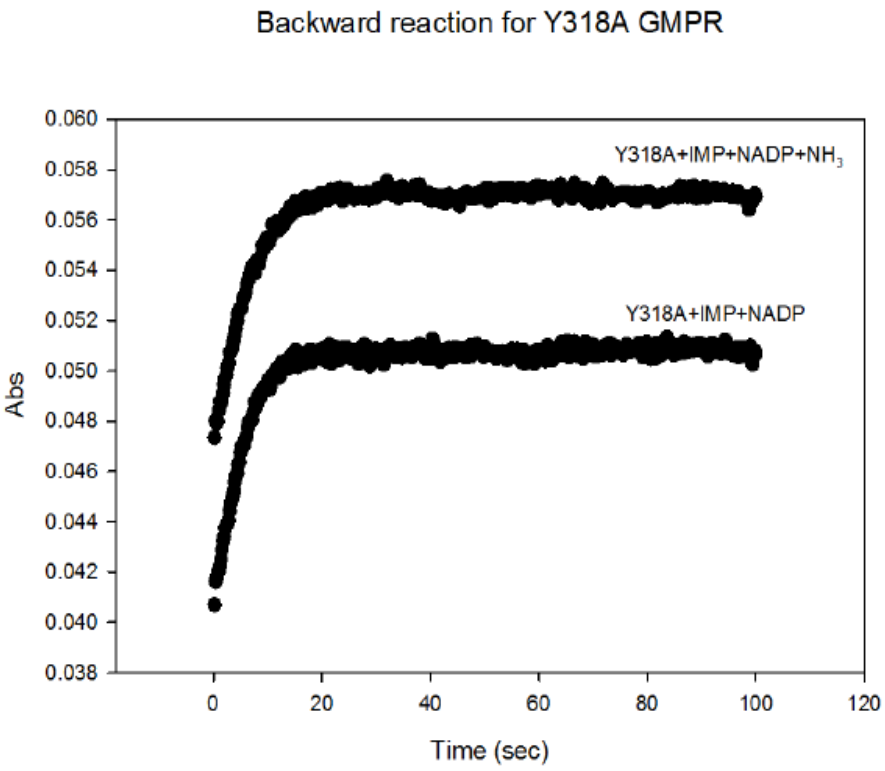

(c) Backward reaction for Y318A GMPR

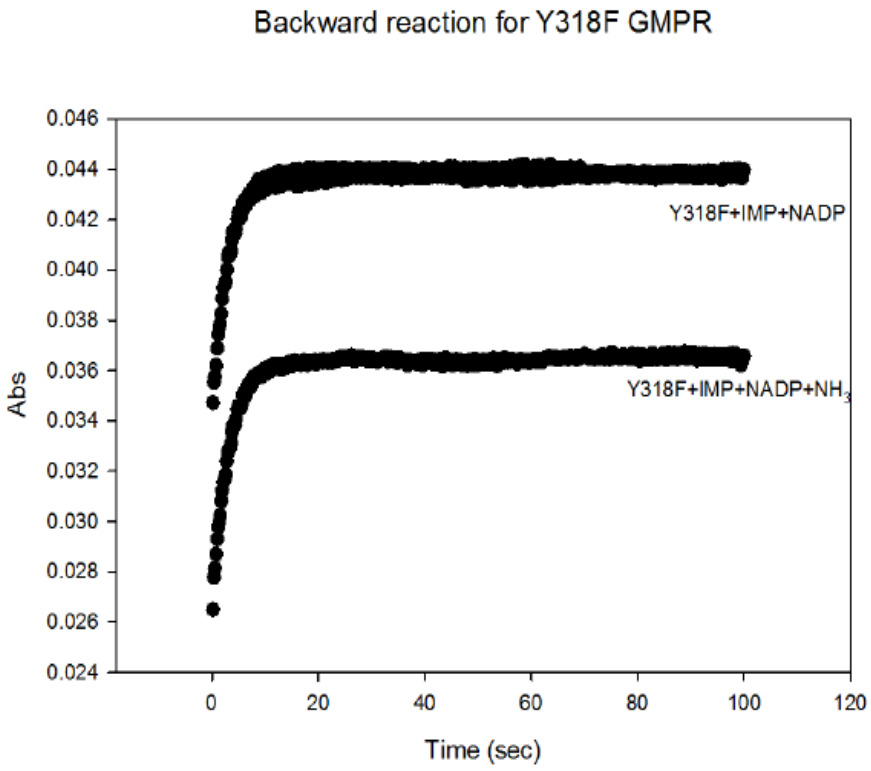

(d) Backward reaction for Y318F GMPR

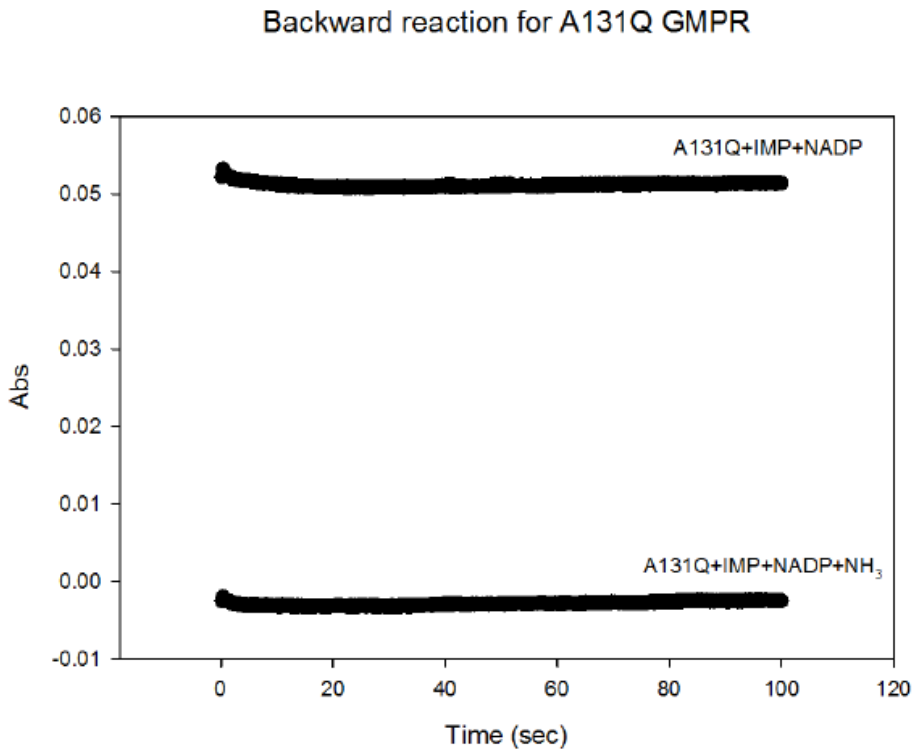

(e) Backward reaction for A131Q GMPR

Figure 7: Backward reaction for WT GMPR and all mutants. 30µL of 1mM indicator (phenol red) is added into 1mL buffer (75mM Tris pH 7.8, 100mM KCl, 1mM EDTA and 1mM DTT). [IMP]=500µM, [NADP] =500µM, [NH_4Cl] =20mM. The absorbance is read at 340nm wavelength for 100 seconds. (a) [WT]=10µM; (b)[T188A]=30µM; (c)[Y318A]=30µM; (d)[Y318F]=10µM; (e)[A131Q]=10µM.

Figure 7 (a) shows the backward reaction curves for WT GMPR in the presence or absence of NH_3. The first order rate constant of exponential phase in the partial backward reaction (without NH_3) is k_p=0.71±0.01 s^{-1}, and in the whole backward reaction (with NH_3) is k_w=0.64±0.01 s^{-1}. There is no big difference between these two first order rate constants. As for the linear phases of both reactions, kcat (whole) =0.018±0.009 s^{-1}, whereas partial reaction reaches plateau meaning that the reaction comes to equilibrium thus kcat (partial) is not relevant. The production of intermediate is 48% relative to enzyme active sites for both partial and whole backward reactions. So from the above information, we can say that

the major difference between partial and whole backward reactions for WT GMPR lies on their linear phases: when adding NH_3, the whole backward reaction will proceed to hydrolysis the intermediate complex thus producing an increasing linear phase; without ammonia, the partial backward reaction will reach a plateau linear phase. Whether having a kcat or not in their linear phases could be used as a direct indicator to show this difference. Meanwhile, they both have very close first order rate constants and intermediate production percentage during their pre-steady state.

Figure 7 (b) shows those two similar shape curves of T188A for partial and whole backward reactions. The first order rate constant of exponential phase in the partial backward reaction (without NH_3) is k_p=0.044±0.001 s^{-1}, and in the whole backward reaction (with NH_3) is k_w=0.033±0.001 s^{-1}, so no big difference between these two values. Both reactions have reached a plateau of which kcat is not relevant indicating that E-XMP* and NADPH are formed but cofactor is not released and E-XMP* is not hydrolyzed in both reactions. Both reactions have an intermediate production of about 3% relative to enzyme active sites. So that means these two curves are almost identical, we can conclude that with or without ammonia, T188A will first form 3% intermediate complex and eventually will reach a plateau. This observation implies that the substitution T188A does affect the backward reaction that causing ammonia not efficiently binding inside enzyme.

Figure 7 (c) shows all results of Y318A for partial and whole backward reactions, and we can almost have the similar conclusion as Figure 7 (b) provided: The first order rate constants of exponential phase for both reactions are very close: k_p=0.20±0.01 s^{-1}, and k_w=0.17±0.01 s^{-1}. Both reactions have reached a plateau of which kcat cannot be calculated because it is not

relevant, and both reactions have an intermediate production of about 10% relative to enzyme active sites. So that means these two curves are almost identical, we can conclude that with or without ammonia, Y318A will first form 10% intermediate complex and will eventually reach a plateau. This observation implies that the substitution Y318A does affect the backward reaction that causing ammonia not efficiently binding inside enzyme. Contrast to this observation, at the same position, a different substitution Y318F shows a different characteristic presented by Figure 7 (d). The first order rate constants of exponential phase for both reactions are almost identical: k_p=0.33±0.01 s^{-1}, and k_w=0.33±0.01 s^{-1}. Both reactions have an intermediate production of about 28% relative to enzyme active sites, however, partial backward reaction reaches a plateau with no detectable kcat after its first burst meanwhile whole backward reaction forms a linear increase after its first burst of which kcat=(4.5±0.5)x10^{-4} s^{-1}. This observation indicates that (i) Tyr318 has a major function for holding ammonia during the reaction; (ii) the aromatic ring is the key reason why this residue can maintain this ammonia holding function. The hydroxyl group may have a minor role in holding ammonia since Y318F does have a 40 fold less kcat in steady stat than WT during the backward reaction, but it is still not significant during the forward reaction. On the other hand, Y318A decreases the kcat in both forward and backward reactions extensively. One explanation for that is: there are several forces between Tyr318 and ammonia for holding ammonia. The force provided by the hydrogen bond between hydroxyl group and ammonia is less important than the force provided by the aromatic ring.

Figure 7 (e) shows that A131Q GMPR cannot produce any intermediate complex for both reactions at all, thus no first order rate constant of exponential phase or kcat of linear

increase phase. There will produce a same amount of intermediate complex with or without NH_3 according to the result of WT GMPR, so the presence of ammonia is not required for the formation of intermediate. Thus, the suggesting role of Gln131 in pushing ammonia away is not a possible explanation. On the other hand, the cofactor is required for both proton uptake assay and partial backward reaction. So another possible role of A131Q is that it may disrupt the correct conformation of cofactor thus blocking the cofactor entering the active site. A131Q has a 50 fold less kcat in forward reaction (than WT) but has no production of intermediate in partial backward reaction, so it probably implies that the substitution A131Q might disrupt the “in” conformation of NADPH, thus causing no production of intermediate in partial backward reaction and lowering the kcat in forward reaction since ammonia release at the end of whole forward reaction.

III. Conclusion:

IMPDH and GMPR have similar structure and both enzymes can catalyze the conversion of IMP to corresponding products. The question about their different reaction specificity remains an interesting topic in biochemistry. One approach to study this reaction specificity is to find out the ammonia holding site in GMPR. We inspected the crystal structure of human GMPR 2 and selected three candidate residues: Thr188, Tyr318 and Ala131. By testing the steady kinetics and pre-steady kinetics of substitutions of these three candidate residues: T188A, Y318A, Y318F, A131Q, we can conclude the following statements:

1. A131Q mutant can carry out the whole forward reaction with a velocity about 50 fold less than WT, but it cannot produce intermediate complex in the hydride transfer step during the backward reaction. This is probably because the longer side chain of this substitution would interrupt the “in” conformation thus blocking the cofactor NADPH from binding to the active site. The field cycling NMR shows that, when enzyme binds to GMP, the inside of enzyme is more dynamic and mobile, this gives the Gln131 more chance to rotate so as to avoid blocking cofactor or pushing away the released ammonia. When enzyme binds to IMP, the inside of enzyme is more rigid and hard to move. So, the longer side chain of Gln131 could have a higher chance to disrupt the “in” conformation by pushing away the ammonia or the cofactor. That’s why this A131Q mutant can proceed the forward reaction but with no production of intermediate in partial or whole backward

reaction.

2. The hypothesis is that, after releasing, ammonia will be held firstly by Thr188 in “out” conformation and then “handed over” to Tyr318 when the cofactor NADPH changes its conformation to “in” conformation. Comparing the results of T188A and Y318A mutants, they are pretty similar and close. Both of them will lower the kcat of forward reaction by a significant level and meanwhile decrease the kcat of backward reaction below detection. They both can form a small burst at the beginning by observation of proton uptake assay and produce an intermediate complex about 4 fold less than WT. By inspecting their crystal structure, we noticed that Thr188 can form a hydrogen bond with released ammonia in “out” conformation but not in “in” conformation, and Tyr318 can form hydrogen bond with released ammonia in “in” conformation but not in “out” conformation. So, the observation and results are consistent to our hypothesis. Both residue Thr188 and Tyr318 have contributed to hold ammonia during the whole GMPR reaction, mutating one of them can partially affect the ammonia releasing rate. Future experiment could focus on double mutation of Thr188 and Tyr318 to see if it will cause an adequate burst of ammonia release.

3. By comparing the results of Y318A and Y318F mutants, we find out that Y318F mutant is more like the WT according to each kinetic parameters and Y318A has a huge different characteristic with respect to Y318F. Y318F has an almost same kcat of forward reaction as WT does; meanwhile the kcat of forward reaction for Y318A is at least 100 fold less than WT. The hydride transfer step is the rate limiting step in both WT and Y318F GMPR, and both WT and Y318F showed a linear increase without any burst at the beginning in proton uptake assay. Also for the backward reaction, Y318F has a linear increase in steady state after

formation of intermediate complex when adding ammonia; however Y318A reaches a plateau which kcat is not relevant and cannot be calculated with or without the presence of ammonia. The main reason cause this difference is the aromatic ring in Tyr318. Comparing to the hydroxyl group in Tyr318, the aromatic ring plays a more significant role in holding ammonia. This observation can provide some insights into how subtle structure changes can cause totally different outcomes. Future experiments could focus on substituting same position residues with similar structure.

IV. Appendices:

Structures for all substrates:

GMP

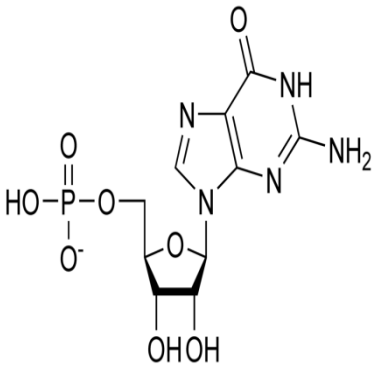

IMP

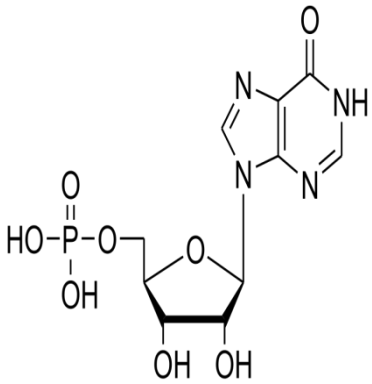

Enzyme kinetics. Standard GMPR assays were conducted at 25^{o}C in 75mM Tris pH 7.8, 100mM KCl, 1mM EDTA and 1mM DTT (GMPR assay buffer). Enzyme activity was monitored spectrophotometrically at 340 nm. Initial velocity data was fit to the Michaelis-Menten equation, where v is the initial velocity, V_m is the maximal velocity, K_m is the Michaelis constant and S is the substrate concentration:

$$v=V_m[S]/(K_m+[S])$$

Primary deuterium isotope effects were determined by varying the concentration of 4S-[^{2}H] NADPH at saturating GMP to determine the values of V_m and V/K_m for NADPH.

Matrix measurement used a different equation: Two Substrate Random Bi-Bi (Sequential)

equation, where v is the initial velocity, V_m is the maximal velocity, A is one substrate concentration, B is other substrate concentration, α is the dissociation constant, Ka is the Michaelis constant for substrate A, Kb is the Michaelis constant for substrate B. The equation shows as follows:

$$v=V_m[A][B]/(\alpha*(Ka*Kb+Kb*[A]+Ka*[B])+[A][B])$$

Stopped-flow kinetics. A stopped-flow spectrophotometer (Applied Photophysics SX.17MV) was used to conduct pre-steady-state experiments. The changing color of indicator (phenol red) in proton uptake assay was monitored by absorbance at 560nm at 25^{o}C; the production of NADPH in partial backward reaction or whole backward reaction was monitored by absorbance at 340nm at 25^{o}C, with a 420nm cut-off filter. For proton uptake assay and backward reaction (both partial and whole reaction), different kinds of GMPR were applied with different concentration: WT=10μM; T188A=30μM; Y318A=30μM; Y318F=10μM; A131Q=10μM. For proton uptake assay, [GMP]=500μM, [NADPH]=500μM ; For backward reactions (both partial and whole reaction), [IMP]=500μM, [$NADP^+$]=500μM, [NH_4^+]=20mM.

Accession codes. Protein Data Bank: The structure of the ternary hGMPR2-IMP-NADPH complex was deposited in the PDB under the accession codes 2C6Q. The software for inspecting the crystal structure was UCSF Chimera.

Bacterial complementation assays. BL21 ΔguaC was transformed with pET28a and pET28a constructs designed to express either *E. coli* GMPR. Cultures were grown overnight in LB

medium with 25μg/ml kanamycin, centrifuged and resuspended in water. Aliquots (5μl) of 1:5 serial dilutions were plated on M9 minimal media containing 0.5% casamino acids, 100μg/ml L-tryptophan, 0.1% thiamin, 25μg/ml kanamycin, and 66μM IPTG. As noted, media were supplemented with 20μg/ml guanosine or xanthine. Plates were incubated at 37°C.

Cloning of the Escherichia coli K12 GMPR gene and mutagenesis. The 1.4-kb guaC gene encoding GMPR from *E. coli* K12 was amplified from a pUC plasmid using pET28a GMPR FP (5'-TGGTGCCTCGTGGTAGCCATATGCGTATTGAAGAAGATCTGAAGTTAGGT-3') and pET28a GMPR RP (5'-CTCAGCTTCCTTTCGGGCTTTGTTACAGGTTGTTGAAGATGCGGTTTTCT-3'). The resulting PCR product was then used in a second PCR with empty pET28a vector to afford pET28a GMPR. Thr188A, Y318A, Y318F and A131Q were cloned out of a pGS682 plasmid using the pET28a GMPR FP and pET28a GMPR RP. The resulting PCR products were utilized in a second PCR with pET28a GMPR as the template to create the mutant plasmids. The generated PCR product was subsequently used as the forward and reverse primers with pET28a GMPR as the template DNA to construct the mutant. Phusion™ Hot Start DNA polymerase was used for all cloning procedures. DNA sequencing of each plasmid revealed the desired sequence.

Expression and purification of *E. coli* GMPR. The endogenous guaC gene of BL21s was knocked out using the procedure described by Warner and coworkers to generate BL21 ΔguaC cells. Transformed BL21 ΔguaC cells containing the appropriate pET28a GMPR

plasmid were grown in LB medium containing 50µg/mL kanamycin and 10µg/mL tetracycline at 37^{o}C and induced with 0.5mM IPTG when the OD_{600nm} reached 0.6. The cells were then grown at 25^{o}C for an additional 22 hours followed by centrifugation at 4^{o}C for 15min at 11,900 x g in a Beckman JLA10.500 rotor. The cell paste was resuspended in GMPR start buffer (50mM Tris, pH 7.8 at 4^{o}C, 100mM KCl, 1mM DTT, 1mM benzamidine, and 10% glycerol) and stored at –80^{o}C. The cell paste was thawed and sonicated on ice for 2 min total [35% Amp, 20.0 s on and 40.0 s off]. After centrifugation at 23,700 x g for 30 min in a Beckman JA20 rotor, the supernatant was filtered through a 0.2µm cellulose acetate filter. The filtered supernatant was loaded at 1mL/min onto a 1mL His Hi Trap column charged with 0.1M NiSO4 and equilibrated in GMPR start buffer on an ATKA FPLC. The affinity column was washed with 5 column volumes GMPR start buffer. The column was washed with 10 column volumes of buffer 1 (75mM Tris, pH 7.8 at 4^{o}C, 100mM KCl, 1mM DTT, and 30mM imidazole). The His column was then washed from 10 column volumes at 75% buffer 1 and 25% buffer 2 (75mM Tris, pH 7.8 at 4^{o}C, 100mM KCl, 1mM DTT, and 500mM imidazole). The protein was eluted over 20 column volumes using gradient from 25% to 100% buffer 2 while collecting 1mL fractions. His6-GMPR containing fractions were identified by absorbance at 280nm and SDS PAGE. Pure His6-GMPR fractions were combined and concentrated on an Amicon Ulta 15 YM10. The protein was dialyzed against 75mM Tris, pH 7.8 at 25^{o}C, 100mM KCl, 1mM EDTA, and 1mM DTT. The protein was stored at –80^{o}C in 10% glycerol. Concentration of protein was determined using Nano drop equipment by applying Lambert-Beer Law.

V. Bibliography:

Gregory C Patton, Pål Stenmark, Deviprasad R Gollapalli, Robin Sevastik, Petri Kursula, Susanne Flodin, Herwig Schuler, Colin T Swales, Hans Eklund, Fahmi Himo, Pär Nordlund, Lizbeth Hedstrom. (2011). Cofactor mobility determines reaction outcome in the IMPDH and GMPR $(\beta\text{-}\alpha)_8$ barrel enzymes. *Nature Chemical Biology, 7*. doi: 10.1038

Lizbeth Hedstrom. (2009). IMP Dehydrogenase: Structure, Mechanism and Inhibition. *Chem Rev., 109*(7), 2903-2928. doi: 10.1021

Lizbeth Hedstrom. (2012). The dynamic determinants of reaction specificity in the IMPDH/GMPR family of $(\beta/\alpha)_8$ barrel enzymes. *Crit Rev Biochem Mol Biol., 47*(3), 250-263. doi: 10.3109

Jia Zhang, Weiping Zhang, Dajin Zou, Guoyou Chen, Tao Wan, Minghui Zhang, Xuetao Cao. (2003). Cloning and functional characterization of GMPR2, a novel human guanosine monophosphate reductase, which promotes the monocytic differentiation of HL-60 leukemia cells. *J Cancer Res Clin Oncol., 129*, 76-83. doi: 10.1007

Jixi Li, Zhiyi Wei, Mei Zheng, Xing Gu, Yingfeng Deng, Rui Qiu, Fei Chen, Chaoneng Ji, Weimin Gong, Yi Xie, Yumin Mao. (2005). Crystal Structure of Human Guanosine Monophosphate Reductase 2 (GMPR2) in Complex with GMP. *J.Mol.Biol., 355*, 980-988. doi: 10.1016

Joseph A. Wawrzyniak, Anna Bianchi-Smiraglia, Wiam Bshara, Sudha Mannava, Jeff Ackroyd, Archis Bagati, Angela R. Omilian, Michael Im, Natalia Fedtsova, Jeffrey C. Miecznikowski, Kalyana C. Moparthy, Shoshanna N. Zucker, Qianqian Zhu, Nadezhda I. Kozlova, Albert E. Berman, Keith S. Hoek, Andrei V. Gudkov, Donna S. Shewach, Carl D. Morrison, Mikhail A. Nikiforov. (2013). A Purine Nucleotide Biosynthesis Enzyme Guanosine Monophosphate Reductase Is a Suppressor of Melanoma Invasion. *Cell Reports, 5*(493-507).